Doping dependence of Meissner effect in cuprate superconductors

Shiping Feng*, Zheyu Huang, and Huaisong Zhao
Department of Physics, Beijing Normal University, Beijing 100875, China

Within the t-t'-J model, the doping dependence of the Meissner effect in cuprate superconductors is studied based on the kinetic energy driven superconducting mechanism. Following the linear response theory, it is shown that the electromagnetic response consists of two parts, the diamagnetic current and the paramagnetic current, which exactly cancels the diamagnetic term in the normal state, and then the Meissner effect is obtained for all the temperature $T \leq T_c$ throughout the superconducting dome. By considering the two-dimensional geometry of cuprate superconductors within the specular reflection model, the main features of the doping and temperature dependence of the local magnetic field profile, the magnetic field penetration depth, and the superfluid density observed on cuprate superconductors are well reproduced. In particular, it is shown that in analogy to the domelike shape of the doping dependent superconducting transition temperature, the maximal superfluid density occurs around the critical doping $\delta \approx 0.195$, and then decreases in both lower doped and higher doped regimes.

PACS numbers: 74.25.Ha, 74.25.Nf, 74.20.Mn

I. INTRODUCTION

One of the characteristic features of superconductors is the so-called Meissner effect[2], i.e., a superconductor is placed in an external magnetic field B smaller than the upper critical field B_c, the magnetic field B penetrates only to a penetration depth λ (few hundred nm for cuprate superconductors at zero-temperature) and is excluded from the main body of the system. This magnetic field penetration depth is a fundamental parameter of superconductors, and is closely related to the superfluid density ρ_s[2,3], which is proportional to the squared amplitude of the macroscopic wave function, and therefore describes the superconducting (SC) charge carriers. Furthermore, the variation of the magnetic field penetration depth (then the superfluid density) as a function of doping and temperature provides information crucial to understanding the details of the SC state[2,3]. In particular, since the compounds of cuprate superconductors are doped Mott insulators with the strong short-range antiferromagnetic correlation dominating the entire SC phase[4], the magnetic field can be also used to probe the doping and momentum dependence of the SC gap and spin structure of the Cooper pair[3]. This is why the first evidence of the d-wave Cooper pairing state in cuprate superconductors was obtained from the earlier experimental measurement for the magnetic field penetration depth[5]. Since then this d-wave SC state remains one of the cornerstones of our understanding of the physics in cuprate superconductors[4,6].

Experimentally, by virtue of systematic studies using the muon-spin-rotation measurement technique, some essential features of the evolution of the magnetic field penetration depth and superfluid density in cuprate superconductors with doping and temperature have been established now for all the temperature $T \leq T_c$ throughout the SC dome: (1) the magnetic field screening is found to be of exponential character[7,8], in support of a local (London-type) nature of the electrodynamic response[2]; (2) the magnetic field penetration depth is a linear temperature dependence at low temperatures except for the extremely low temperatures where a strong deviation from the linear characteristics (a nonlinear effect) appears[5,9–11]; (3) the doping dependence of the superfluid density is observed[12–15], where the superfluid density exhibits a peak around the critical doping $\delta \approx 0.19$, and then decreases at both lower doped and higher doped regimes. This in turn gives rise to the domelike shape of the doping dependence of the SC transition temperature. In particular, it has been shown experimentally[13] that the peak of the superfluid density at the critical doping $\delta \approx 0.19$ is a common feature of the hole-doped cuprate superconductors. Theoretically, to the best of our knowledge, all theoretical calculations of the experimental measurements of the magnetic field penetration depth and the related superfluid density in cuprate superconductors performed so far are based on the phenomenological d-wave Bardeen-Cooper-Schrieffer (BCS) formalism[16–20]. In the local limit, where the magnetic field penetration depth λ is much larger than the coherence length ζ, i.e., $\lambda \gg \zeta$, it has been shown[6,17] that the simple d-wave pairing state gives the linear temperature dependence of the magnetic field penetration depth $\Delta\lambda(T) = \lambda(T) - \lambda(0) \propto T/\Delta_0$ at low temperatures, with Δ_0 is the zero-temperature value of the d-wave gap amplitude. However, the characteristic feature of the d-wave energy gap is the existence of the gap nodes on the Fermi surface, which can lead to the nonlinear effect of field on the penetration depth (then superfluid density) at the extremely low temperatures, associated with a field induced increase in the density of available excitation states located around the gap nodes on the Fermi surface[16–20]. This follows from a fact that the nonlocal effect is closely related to the divergence of the coherence length ζ at the gap nodes on the Fermi surface, as the coherence length ζ varies in inverse proportion to the value of the energy gap, then this nonlocal effect at the extremely low temperatures can lead to a nonlinear temperature depen-

dence of the magnetic field penetration depth in the clean limit[16–20].

In our recent work[21] based on the nearest neighbors hopping t-J model, the weak electromagnetic response in cuprate superconductors has been discussed within the kinetic energy driven SC mechanism[22]. However, it has been shown experimentally[4,23] that although the highest energy filled electron band is well described by the nearest neighbors hopping t-J model, the overall dispersion may be properly accounted by generalizing the nearest neighbors hopping t-J model to include the second- and third-nearest neighbors hopping terms t' and t''. Furthermore, the experimental analysis[24] showed that the SC transition temperature (then the superfluid density) for different families of cuprate superconductors is strongly correlated with t'. In this paper based on the t-t'-J model, we study the doping dependence of the Meissner effect in cuprate superconductors for all the temperature $T \leq T_c$ throughout the SC dome, where one of our main results is that the superfluid density increases with increasing doping in the lower doped regime, and reaches a maximum around the critical doping $\delta \approx 0.195$, then decreases in the higher doped regime.

The rest of this paper is organized as follows. The basic formalism is presented in Section II, where within the t-t'-J model, we evaluate the diamagnetic and paramagnetic components of the response kernel function based on the kinetic energy driven SC mechanism, and then obtain explicitly the Meissner effect in cuprate superconductors for all the temperature $T \leq T_c$ throughout the SC dome. Within this theoretical framework, we discuss the basic behavior of cuprate superconductors in a weak electromagnetic field in Section III, and qualitatively reproduce all the main features of the doping and temperature dependence of the local magnetic field profile, the magnetic field penetration depth, and the superfluid density. Finally, we give a summary and discussions in Section IV. In Appendix A we give the explicit forms of the paramagnetic part of the response kernel function at the temperatures $T = 0$ and $T = T_c$, respectively.

II. THEORETICAL FRAMEWORK

In cuprate superconductors, the characteristic feature is the presence of the CuO_2 plane[4]. It has been argued that the essential physics of the doped CuO_2 plane[4,25] is properly accounted by the t-t'-J model on a square lattice. However, for discussions of the doping and temperature dependence of the Meissner effect in cuprate superconductors, the t-t'-J model can be extended by including the exponential Peierls factors as,

$$\begin{aligned} H &= -t\sum_{l\hat{\eta}\sigma} e^{-i(e/\hbar)\mathbf{A}(l)\cdot\hat{\eta}} C^{\dagger}_{l\sigma} C_{l+\hat{\eta}\sigma} + \mu \sum_{l\sigma} C^{\dagger}_{l\sigma} C_{l\sigma} \\ &+ t'\sum_{l\hat{\eta}'\sigma} e^{-i(e/\hbar)\mathbf{A}(l)\cdot\hat{\eta}'} C^{\dagger}_{l\sigma} C_{l+\hat{\eta}'\sigma} + J\sum_{l\hat{\eta}} \mathbf{S}_l \cdot \mathbf{S}_{l+\hat{\eta}}, \quad (1) \end{aligned}$$

supplemented by an important on-site local constraint $\sum_{\sigma} C^{\dagger}_{l\sigma} C_{l\sigma} \leq 1$ to remove the double occupancy, where $\hat{\eta} = \pm\hat{x}, \pm\hat{y}$, $\hat{\eta}' = \pm\hat{x} \pm \hat{y}$, $C^{\dagger}_{l\sigma}$ ($C_{l\sigma}$) is the electron creation (annihilation) operator, $\mathbf{S}_l = (S^x_l, S^y_l, S^z_l)$ are spin operators, and μ is the chemical potential. The exponential Peierls factors account for the coupling of electrons to the weak external magnetic field[26,27] in terms of the vector potential $\mathbf{A}(l)$. To incorporate the electron single occupancy local constraint, the charge-spin separation (CSS) fermion-spin theory[28] has been proposed, where the physics of no double occupancy is taken into account by representing the electron as a composite object created by $C_{l\uparrow} = h^{\dagger}_{l\uparrow} S^{-}_{l}$ and $C_{l\downarrow} = h^{\dagger}_{l\downarrow} S^{+}_{l}$, with the spinful fermion operator $h_{l\sigma} = e^{-i\Phi_{l\sigma}} h_l$ that describes the charge degree of freedom of the electron together with some effects of spin configuration rearrangements due to the presence of the doped hole itself (charge carrier), while the spin operator S_l represents the spin degree of freedom of the electron, then the electron single occupancy local constraint is satisfied in analytical calculations. In particular, it has been shown that under the *decoupling scheme*, this CSS fermion-spin representation is a natural representation of the constrained electron defined in the Hilbert subspace without double electron occupancy[29]. In this CSS fermion-spin representation, the t-t'-J model (1) can be expressed as,

$$\begin{aligned} H &= t\sum_{l\hat{\eta}} e^{-i(e/\hbar)\mathbf{A}(l)\cdot\hat{\eta}} (h^{\dagger}_{l+\hat{\eta}\uparrow} h_{l\uparrow} S^{+}_{l} S^{-}_{l+\hat{\eta}} \\ &+ h^{\dagger}_{l+\hat{\eta}\downarrow} h_{l\downarrow} S^{-}_{l} S^{+}_{l+\hat{\eta}}) \\ &- t'\sum_{l\hat{\eta}'} e^{-i(e/\hbar)\mathbf{A}(l)\cdot\hat{\eta}'} (h^{\dagger}_{l+\hat{\eta}'\uparrow} h_{l\uparrow} S^{+}_{l} S^{-}_{l+\hat{\eta}'} \\ &+ h^{\dagger}_{l+\hat{\eta}'\downarrow} h_{l\downarrow} S^{-}_{l} S^{+}_{l+\hat{\eta}'}) \\ &- \mu\sum_{l\sigma} h^{\dagger}_{l\sigma} h_{l\sigma} + J_{\rm eff}\sum_{l\hat{\eta}} \mathbf{S}_l \cdot \mathbf{S}_{l+\hat{\eta}}, \quad (2) \end{aligned}$$

where $J_{\rm eff} = (1-\delta)^2 J$, and $\delta = \langle h^{\dagger}_{l\sigma} h_{l\sigma}\rangle = \langle h^{\dagger}_{l} h_{l}\rangle$ is the charge carrier doping concentration.

As in the conventional superconductors, the key phenomenon occurring in cuprate superconductors in the SC state is the pairing of charge carriers[4,6]. The system of charge carriers forms pairs of bound charge carriers in the SC state, while the pairing means that there is an attraction between charge carriers. What is the origin of such an attractive force? Recently, the kinetic energy driven SC mechanism has been developed based on the t-J model[22], where the charge carrier-spin interaction from the kinetic energy term in the t-J model (2) induces a d-wave charge carrier pairing state by exchanging spin excitations in the higher power of the doping concentration, then the SC transition temperature is identical to the charge carrier pair transition temperature. Furthermore, this SC state is the conventional BCS-like with the d-wave symmetry[29,30], so that the basic d-wave BCS formalism is still valid in quantitatively reproducing all main low energy features of the SC co-

herence of the quasiparticle peaks in cuprate superconductors, although the pairing mechanism is driven by the kinetic energy by exchanging spin excitations. Following these previous discussions[22,29,30], the full charge carrier Green's function in the zero magnetic field case can be obtained explicitly in the Nambu representation as,

$$\mathbb{G}(\mathbf{k}, i\omega_n) = Z_{\rm hF}\, \frac{i\omega_n\tau_0 + \bar{\xi}_{\mathbf{k}}\tau_3 - \bar{\Delta}_{\rm hZ}(\mathbf{k})\tau_1}{(i\omega_n)^2 - E^2_{{\rm h}\mathbf{k}}}, \tag{3}$$

where τ_0 is the unit matrix, τ_1 and τ_3 are Pauli matrices, the renormalized charge carrier excitation spectrum $\bar{\xi}_{\mathbf{k}} = Z_{\rm hF}\xi_{\mathbf{k}}$, with the mean-field charge carrier excitation spectrum $\xi_{\mathbf{k}} = Zt\chi_1\gamma_{\mathbf{k}} - Zt'\chi_2\gamma'_{\mathbf{k}} - \mu$, the spin correlation functions $\chi_1 = \langle S^+_i S^-_{i+\hat{\eta}}\rangle$, $\chi_2 = \langle S^+_i S^-_{i+\hat{\eta}'}\rangle$, $\gamma_{\mathbf{k}} = (1/Z)\sum_{\hat{\eta}} e^{i\mathbf{k}\cdot\hat{\eta}}$, $\gamma'_{\mathbf{k}} = (1/Z)\sum_{\hat{\eta}'} e^{i\mathbf{k}\cdot\hat{\eta}'}$, Z is the number of the nearest neighbor or second-nearest neighbor sites, the renormalized charge carrier d-wave pair gap $\bar{\Delta}_{\rm hZ}(\mathbf{k}) = Z_{\rm hF}\bar{\Delta}_{\rm h}(\mathbf{k})$, where the effective charge carrier d-wave pair gap $\bar{\Delta}_{\rm h}(\mathbf{k}) = \bar{\Delta}_{\rm h}(\cos k_x - \cos k_y)/2$, and the charge carrier quasiparticle spectrum $E_{{\rm h}\mathbf{k}} = \sqrt{\bar{\xi}^2_{\mathbf{k}} + |\bar{\Delta}_{\rm hZ}(\mathbf{k})|^2}$, while the effective charge carrier gap parameter $\bar{\Delta}_{\rm h}$ and the quasiparticle coherent weight $Z_{\rm hF}$ have been determined self-consistently along with other equations[29,30], and then all order parameters and chemical potential have been determined by the self-consistent calculation.

A. Linear response approach in the presence of a weak external magnetic field

In cuprate superconductors, an external magnetic field generally represents a large perturbation on the system, then the induced field arising from the superconductor cancels this external magnetic field over most of the system. In this case, the net field acts only near the surface on a scale of the magnetic field penetration depth, and then it can be treated as a weak perturbation on the system as a whole[2]. This is why the Meissner effect can be successfully studied within the linear response approach[31,32], where the linear response current density J_μ and the vector potential A_ν are related by a nonlocal kernel of the response function $K_{\mu\nu}$ as,

$$J_\mu(\mathbf{q},\omega) = -\sum_{\nu=1}^{3} K_{\mu\nu}(\mathbf{q},\omega)A_\nu(\mathbf{q},\omega), \tag{4}$$

with the Greek indices label the axes of the Cartesian coordinate system. The kernel of the response function in Eq. (4) plays a crucial role for the discussion of the doping dependence of the Meissner effect in cuprate superconductors, and can be separated into two parts as,

$$K_{\mu\nu}(\mathbf{q},\omega) = K^{(\rm d)}_{\mu\nu}(\mathbf{q},\omega) + K^{(\rm p)}_{\mu\nu}(\mathbf{q},\omega), \tag{5}$$

where $K^{(\rm d)}_{\mu\nu}$ and $K^{(\rm p)}_{\mu\nu}$ are the corresponding diamagnetic and paramagnetic parts, respectively, and are closely related to the electron current density in the presence of the vector potential A_ν.

The vector potential $\mathbf{A}$ (then the weak external magnetic field $\mathbf{B} = {\rm rot}\,\mathbf{A}$) has been coupled to the electrons, which are now represented by $C_{l\uparrow} = h^\dagger_{l\uparrow}S^-_l$ and $C_{l\downarrow} = h^\dagger_{l\downarrow}S^+_l$ in the CSS fermion-spin representation. In this case, the electron current operator can be obtained in terms of the electron polarization operator, which is a summation over all the particles and their positions, and can be expressed explicitly in the CSS fermion-spin representation as,

$$\mathbf{P} = -e\sum_{i\sigma}\mathbf{R}_i C^\dagger_{i\sigma}C_{i\sigma} = e\sum_i \mathbf{R}_i h^\dagger_i h_i, \tag{6}$$

then the electron current operator is obtained by evaluating the time-derivative of this polarization operator (6) as[33],

$$\begin{aligned}
\mathbf{j} &= \frac{\partial\mathbf{P}}{\partial t} = \frac{i}{\hbar}[H,\mathbf{P}] \\
&= \frac{iet}{\hbar}\sum_{l\hat{\eta}}\hat{\eta}e^{-i(\frac{e}{\hbar})\mathbf{A}(l)\cdot\hat{\eta}}\Big(h_{l\uparrow}h^\dagger_{l+\hat{\eta}\uparrow}S^+_l S^-_{l+\hat{\eta}} \\
&+ h_{l\downarrow}h^\dagger_{l+\hat{\eta}\downarrow}S^-_l S^+_{l+\hat{\eta}}\Big) \\
&- \frac{iet'}{\hbar}\sum_{l\hat{\eta}'}\hat{\eta}'e^{-i(\frac{e}{\hbar})\mathbf{A}(l)\cdot\hat{\eta}'}\Big(h_{l\uparrow}h^\dagger_{l+\hat{\eta}'\uparrow}S^+_l S^-_{l+\hat{\eta}'} \\
&+ h_{l\downarrow}h^\dagger_{l+\hat{\eta}'\downarrow}S^-_l S^+_{l+\hat{\eta}'}\Big).
\end{aligned} \tag{7}$$

In the linear response approach, this electron current operator is reduced as $\mathbf{j} = \mathbf{j}^{(d)} + \mathbf{j}^{(p)}$, with the corresponding diamagnetic (d) and paramagnetic (p) components of the electron current operator are given by,

$$\begin{aligned}
\mathbf{j}^{(\rm d)} &= \frac{e^2t}{\hbar^2}\sum_{l\hat{\eta}}\hat{\eta}\mathbf{A}(l)\cdot\hat{\eta}\Big(h_{l\uparrow}h^\dagger_{l+\hat{\eta}\uparrow}S^+_l S^-_{l+\hat{\eta}} \\
&+ h_{l\downarrow}h^\dagger_{l+\hat{\eta}\downarrow}S^-_l S^+_{l+\hat{\eta}}\Big) \\
&- \frac{e^2t'}{\hbar^2}\sum_{l\hat{\eta}'}\hat{\eta}'\mathbf{A}(l)\cdot\hat{\eta}'\Big(h_{l\uparrow}h^\dagger_{l+\hat{\eta}'\uparrow}S^+_l S^-_{l+\hat{\eta}'} \\
&+ h_{l\downarrow}h^\dagger_{l+\hat{\eta}'\downarrow}S^-_l S^+_{l+\hat{\eta}'}\Big),
\end{aligned} \tag{8a}$$

$$\begin{aligned}
\mathbf{j}^{(\rm p)} &= \frac{iet}{\hbar}\sum_{l\hat{\eta}}\hat{\eta}\Big(h_{l\uparrow}h^\dagger_{l+\hat{\eta}\uparrow}S^+_l S^-_{l+\hat{\eta}} + h_{l\downarrow}h^\dagger_{l+\hat{\eta}\downarrow}S^-_l S^+_{l+\hat{\eta}}\Big) \\
&- \frac{iet'}{\hbar}\sum_{l\hat{\eta}'}\hat{\eta}'\Big(h_{l\uparrow}h^\dagger_{l+\hat{\eta}'\uparrow}S^+_l S^-_{l+\hat{\eta}'} \\
&+ h_{l\downarrow}h^\dagger_{l+\hat{\eta}'\downarrow}S^-_l S^+_{l+\hat{\eta}'}\Big),
\end{aligned} \tag{8b}$$

respectively. Obviously, the diamagnetic component of the electron current operator in Eq. (8a) is proportional to the vector potential, and in this case, we can obtain the diamagnetic part of the response kernel directly as,

$$K^{(\rm d)}_{\mu\nu}(\mathbf{q},\omega) = -\frac{4e^2}{\hbar^2}(\chi_1\phi_1 t - 2\chi_2\phi_2 t')\delta_{\mu\nu} = \frac{1}{\lambda^2_L}\delta_{\mu\nu}, \tag{9}$$

where the charge carrier particle-hole parameters $\phi_1 = \langle h^{\dagger}_{i\sigma} h_{i+\hat{\eta}\sigma}\rangle$ and $\phi_2 = \langle h^{\dagger}_{i\sigma} h_{i+\hat{\eta}'\sigma}\rangle$, while $\lambda_L^{-2} = -4e^2(\chi_1\phi_1 t - 2\chi_2\phi_2 t')/\hbar^2$ is the London penetration depth, and is doping and temperature dependent.

However, the paramagnetic part of the response kernel is more complicated to calculate, since it involves evaluation of the following electron current-current correlation function (polarization bubble),

$$P_{\mu\nu}(\mathbf{q},\tau) = -\langle T_\tau\{j^{(\mathrm{p})}_\mu(\mathbf{q},\tau) j^{(\mathrm{p})}_\nu(-\mathbf{q},0)\}\rangle, \tag{10}$$

then the paramagnetic part of the response kernel $K^{(\mathrm{p})}_{\mu\nu}(\mathbf{q},\omega)$ can be obtained as $K^{(\mathrm{p})}_{\mu\nu}(\mathbf{q},\omega) = P_{\mu\nu}(\mathbf{q},\omega)$. In the CSS fermion-spin approach, the paramagnetic component of the electron current operator in Eq. (8b) can be decoupled as,

$$\begin{aligned}
\mathbf{j}^{(\mathrm{p})} &= -\frac{ie\chi_1 t}{\hbar}\sum_{l\hat{\eta}\sigma}\hat{\eta} h^{\dagger}_{l+\hat{\eta}\sigma} h_{l\sigma} + \frac{ie\chi_2 t'}{\hbar}\sum_{l\hat{\eta}'\sigma}\hat{\eta}' h^{\dagger}_{l+\hat{\eta}'\sigma} h_{l\sigma} \\
&- \frac{ie\phi_1 t}{\hbar}\sum_{l\hat{\eta}}\hat{\eta}\left(S^{+}_{l} S^{-}_{l+\hat{\eta}} + S^{-}_{l} S^{+}_{l+\hat{\eta}}\right) \\
&+ \frac{ie\phi_2 t'}{\hbar}\sum_{l\hat{\eta}'}\hat{\eta}'\left(S^{+}_{l} S^{-}_{l+\hat{\eta}'} + S^{-}_{l} S^{+}_{l+\hat{\eta}'}\right),
\end{aligned} \tag{11}$$

where the third and fourth terms in the right-hand side refer to the contribution from the electron spin, and can be expressed explicitly as,

$$\begin{aligned}
&- \frac{ie\phi_1 t}{\hbar}\sum_{l\hat{\mu}}\hat{\mu}[(S^{+}_{l} S^{-}_{l+\hat{\mu}} + S^{-}_{l} S^{+}_{l+\hat{\mu}}) - (S^{+}_{l} S^{-}_{l-\hat{\mu}} + S^{-}_{l} S^{+}_{l-\hat{\mu}})] = \frac{ie\phi_1 t}{\hbar}\sum_{l\hat{\mu}}\hat{\mu}[(S^{+}_{l+\hat{\mu}} S^{-}_{l} + S^{-}_{l+\hat{\mu}} S^{+}_{l}) - (S^{+}_{l} S^{-}_{l+\hat{\mu}} + S^{-}_{l} S^{+}_{l+\hat{\mu}})] \\
&\equiv 0, \\
&\frac{ie\phi_2 t'}{\hbar}\sum_{l}[(\hat{x}+\hat{y})(S^{+}_{l} S^{-}_{l+\hat{x}+\hat{y}} + S^{-}_{l} S^{+}_{l+\hat{x}+\hat{y}}) - (\hat{x}+\hat{y})(S^{+}_{l} S^{-}_{l-\hat{x}-\hat{y}} + S^{-}_{l} S^{+}_{l-\hat{x}-\hat{y}}) + (\hat{x}-\hat{y})(S^{+}_{l} S^{-}_{l+\hat{x}-\hat{y}} + S^{-}_{l} S^{+}_{l+\hat{x}-\hat{y}}) \\
&- (\hat{x}-\hat{y})(S^{+}_{l} S^{-}_{l-\hat{x}+\hat{y}} + S^{-}_{l} S^{+}_{l-\hat{x}+\hat{y}})] \\
&= \frac{ie\phi_2 t'}{\hbar}\sum_{l}[(\hat{x}+\hat{y})(S^{+}_{l} S^{-}_{l+\hat{x}+\hat{y}} + S^{-}_{l} S^{+}_{l+\hat{x}+\hat{y}}) - (\hat{x}+\hat{y})(S^{+}_{l+\hat{x}+\hat{y}} S^{-}_{l} + S^{-}_{l+\hat{x}+\hat{y}} S^{+}_{l}) + (\hat{x}-\hat{y})(S^{+}_{l} S^{-}_{l+\hat{x}-\hat{y}} + S^{-}_{l} S^{+}_{l+\hat{x}-\hat{y}}) \\
&- (\hat{x}-\hat{y})(S^{+}_{l+\hat{x}-\hat{y}} S^{-}_{l} + S^{-}_{l+\hat{x}-\hat{y}} S^{+}_{l})] \equiv 0.
\end{aligned}$$

In this case, the majority contribution for the paramagnetic component of the electron current operator comes from the electron charge, and then the paramagnetic component of the electron current operator in Eq. (11) can be expressed explicitly as,

$$\begin{aligned}
j^{(\mathrm{p})}_\mu &= -\frac{ie\chi_1 t}{\hbar}\sum_{l\sigma}(h^{\dagger}_{l+\hat{\mu}\sigma} h_{l\sigma} - h^{\dagger}_{l\sigma} h_{l+\hat{\mu}\sigma}) \\
&+ \frac{ie\chi_2 t'}{\hbar}\sum_{l\sigma\nu\neq\mu}[(h^{\dagger}_{l+\hat{\mu}+\hat{\nu}\sigma} + h^{\dagger}_{l+\hat{\mu}-\hat{\nu}\sigma}) h_{l\sigma} \\
&- h^{\dagger}_{l\sigma}(h_{l+\hat{\mu}+\hat{\nu}\sigma} + h_{l+\hat{\mu}-\hat{\nu}\sigma})].
\end{aligned} \tag{12}$$

For the convenience in the following discussions, the paramagnetic component of the electron current operator can be rewritten in the Nambu representation in terms of the charge carrier Nambu operators $\Psi^{\dagger}_{\mathbf{k}} = \left(h^{\dagger}_{\mathbf{k}\uparrow}, h_{-\mathbf{k}\downarrow}\right)$ and $\Psi_{\mathbf{k}+\mathbf{q}} = \left(h_{\mathbf{k}+\mathbf{q}\uparrow}, h^{\dagger}_{-\mathbf{k}-\mathbf{q}\downarrow}\right)^T$. Moreover, since the density operator is summed over the position of all particles, then its Fourier transform can be obtained as $\rho(\mathbf{q}) = (e/2)\sum_{\mathbf{k}\sigma} h^{\dagger}_{\mathbf{k}\sigma} h_{\mathbf{k}+\mathbf{q}\sigma} = (e/2)\sum_{\mathbf{k}} \Psi^{\dagger}_{\mathbf{k}}\tau_3\Psi_{\mathbf{k}+\mathbf{q}}$. In this Nambu representation, the paramagnetic four-current operator can be represented as,

$$j^{(p)}_\mu(\mathbf{q}) = \frac{1}{N}\sum_{\mathbf{k}\sigma}\Psi^{\dagger}_{\mathbf{k}}\gamma_\mu(\mathbf{k},\mathbf{k}+\mathbf{q})\Psi_{\mathbf{k}+\mathbf{q}}. \tag{13}$$

where the bare current vertex,

$$\gamma_\mu(\mathbf{k}+\mathbf{q},\mathbf{k}) = \begin{cases} -\frac{2e}{\hbar}\, e^{\frac{1}{2}iq_\mu}\{\sin(k_\mu+\frac{1}{2}q_\mu)[\chi_1 t - 2\chi_2 t'\sum\limits_{\nu\neq\mu}\cos(\frac{1}{2}q_\nu)\cos(k_\nu+\frac{1}{2}q_\nu)] \\ -i(2\chi_2 t')\cos(k_\mu+\frac{1}{2}q_\mu)\sum\limits_{\nu\neq\mu}\sin q_\nu \sin(k_\nu+\frac{1}{2}q_\nu)\}\tau_0 & \text{for } \mu\neq 0, \\ \frac{e}{2}\tau_3 & \text{for } \mu = 0. \end{cases} \tag{14}$$

As in the previous discussions[21], we are calculating the polarization bubble with the paramagnetic current operator (13), i.e., bare current vertices (14), but Green function (3). As a consequence, we do not take into account longitudinal excitations properly[2,27], the obtained results are valid only in the gauge, where the vector potential is purely transverse, e.g. in the Coulomb gauge. In this case, the correlation function (10) can be obtained in the Nambu representation as,

$$P_{\mu\nu}(\mathbf{q},i\omega_n) = \frac{1}{N}\sum_{\mathbf{k}}\gamma_{\mu}(\mathbf{k}+\mathbf{q},\mathbf{k})\gamma^{*}_{\nu}(\mathbf{k}+\mathbf{q},\mathbf{k})\frac{1}{\beta}\sum_{i\nu_m}\mathrm{Tr}\left[\mathbb{G}(\mathbf{k}+\mathbf{q},i\omega_n+i\nu_m)\mathbb{G}(\mathbf{k},i\nu_m)\right]. \tag{15}$$

Substituting the Green's function (3) into Eq. (15), we then obtain the paramagnetic part of the response kernel in the static limit ($\omega\sim 0$) as,

$$K^{(\mathrm{p})}_{\mu\nu}(\mathbf{q},0) = \frac{1}{N}\sum_{\mathbf{k}}\gamma_{\mu}(\mathbf{k}+\mathbf{q},\mathbf{k})\gamma^{*}_{\nu}(\mathbf{k}+\mathbf{q},\mathbf{k})[L_1(\mathbf{k},\mathbf{q})+L_2(\mathbf{k},\mathbf{q})] = K^{(\mathrm{p})}_{\mu\mu}(\mathbf{q},0)\delta_{\mu\nu}, \tag{16}$$

with the functions $L_1(\mathbf{k},\mathbf{q},\omega)$ and $L_2(\mathbf{k},\mathbf{q},\omega)$ are given by,

$$L_1(\mathbf{k},\mathbf{q}) = Z^2_{\mathrm{hF}}\left(1+\frac{\bar{\xi}_{\mathbf{k}+\mathbf{q}}\bar{\xi}_{\mathbf{k}}+\bar{\Delta}_{\mathrm{hZ}}(\mathbf{k}+\mathbf{q})\bar{\Delta}_{\mathrm{hZ}}(\mathbf{k})}{E_{\mathrm{h}\mathbf{k}}E_{\mathrm{h}\mathbf{k}+\mathbf{q}}}\right)\frac{n_{\mathrm{F}}(E_{\mathrm{h}\mathbf{k}})-n_{\mathrm{F}}(E_{\mathrm{h}\mathbf{k}+\mathbf{q}})}{E_{\mathrm{h}\mathbf{k}}-E_{\mathrm{h}\mathbf{k}+\mathbf{q}}}, \tag{17a}$$

$$L_2(\mathbf{k},\mathbf{q}) = Z^2_{\mathrm{hF}}\left(1-\frac{\bar{\xi}_{\mathbf{k}+\mathbf{q}}\bar{\xi}_{\mathbf{k}}+\bar{\Delta}_{\mathrm{hZ}}(\mathbf{k}+\mathbf{q})\bar{\Delta}_{\mathrm{hZ}}(\mathbf{k})}{E_{\mathrm{h}\mathbf{k}}E_{\mathrm{h}\mathbf{k}+\mathbf{q}}}\right)\frac{n_{\mathrm{F}}(E_{\mathrm{h}\mathbf{k}})+n_{\mathrm{F}}(E_{\mathrm{h}\mathbf{k}+\mathbf{q}})-1}{E_{\mathrm{h}\mathbf{k}}+E_{\mathrm{h}\mathbf{k}+\mathbf{q}}}, \tag{17b}$$

respectively. In this case, the kernel of the response function in Eq. (5) is now obtained from Eqs. (9) and (16) as,

$$K_{\mu\nu}(\mathbf{q},0) = \left[\frac{1}{\lambda^2_L}+K^{(\mathrm{p})}_{\mu\mu}(\mathbf{q},0)\right]\delta_{\mu\nu}. \tag{18}$$

It should be emphasized that in the present CSS fermion-spin theory[28,29], these charge carrier $h^{\dagger}_{l\sigma}$ and spin $\mathbf{S}_l$ are gauge invariant, and in this sense they are real and can be interpreted as physical excitations[34]. Furthermore, as shown in Eq. (6) and Eq. (12), the electron polarization operator and the related electron current operator are identified with the corresponding charge carrier polarization operator and charge carrier current operator, since the electron single occupancy local constraint is satisfied in the CSS fermion-spin approach.

B. Doping dependence of the Meissner effect in the long wavelength limit

With the help of the response kernel function (18), we now discuss the doping and temperature dependence of the Meissner effect in cuprate superconductors. In particular, in the long wavelength limit, i.e., $|\mathbf{q}|\rightarrow 0$, the function $L_2(\mathbf{k},\mathbf{q}\rightarrow 0)$ vanishes, then the paramagnetic part of the response kernel can be obtained explicitly as,

$$K^{(\mathrm{p})}_{yy}(\mathbf{q}\rightarrow 0,0) = 2Z^2_{\mathrm{hF}}\frac{4e^2}{\hbar^2}\frac{1}{N}\sum_{\mathbf{k}}\sin^2 k_y[\chi_1 t-2\chi_2 t'\cos k_x]^2\lim_{\mathbf{q}\rightarrow 0}\frac{n_{\mathrm{F}}(E_{\mathrm{h}\mathbf{k}})-n_{\mathrm{F}}(E_{\mathrm{h}\mathbf{k}+\mathbf{q}})}{E_{\mathrm{h}\mathbf{k}}-E_{\mathrm{h}\mathbf{k}+\mathbf{q}}}. \tag{19}$$

At zero-temperature $T=0$, $K^{(\mathrm{p})}_{yy}(\mathbf{q}\rightarrow 0,0)|_{T=0}=0$ (see Appendix A). In this case, the long wavelength electromagnetic response is determined by the diamagnetic part of the kernel only. On the other hand, at the SC transition temperature $T=T_c$, the effective charge carrier gap parameter $\bar{\Delta}_{\mathrm{h}}|_{T=T_c}=0$. In this case, the paramagnetic part of the response kernel in the long wavelength limit can be evaluated as (see Appendix A),

$$K^{(\mathrm{p})}_{yy}(\mathbf{q}\rightarrow 0,0)|_{T=T_c} = 2Z^2_{\mathrm{hF}}\frac{4e^2}{\hbar^2}\frac{1}{N}\sum_{\mathbf{k}}\sin^2 k_y[\chi_1 t-2\chi_2 t'\cos k_x]^2\lim_{\mathbf{q}\rightarrow 0}\frac{n_{\mathrm{F}}(\bar{\xi}_{\mathbf{k}})-n_{\mathrm{F}}(\bar{\xi}_{\mathbf{k}+\mathbf{q}})}{\bar{\xi}_{\mathbf{k}}-\bar{\xi}_{\mathbf{k}+\mathbf{q}}} = -\frac{1}{\lambda^2_L}, \tag{20}$$

which exactly cancels the diamagnetic part of the response kernel (9), and then the Meissner effect in cuprate superconductors is obtained for all $T \leq T_c$. To show this point clearly, we define the effective superfluid density $n_s(T)$ at temperature T in terms of the paramagnetic part of the response kernel as,

$$K_{\mu\nu}^{(\mathrm{p})}(\mathbf{q} \to 0, 0) = -\frac{1}{\lambda_L^2}\left[1 - \frac{n_s(T)}{n_s(0)}\right]\delta_{\mu\nu}, \tag{21}$$

and then the kernel of the response function in Eq. (18) can be rewritten as,

$$K_{\mu\nu}(\mathbf{q} \to 0, 0) = \frac{1}{\lambda_L^2}\frac{n_s(T)}{n_s(0)}\delta_{\mu\nu}, \tag{22}$$

where the ratio $n_s(T)/n_s(0)$ of the effective superfluid densities at temperature T and zero-temperature is given by,

$$\frac{n_s(T)}{n_s(0)} = 1 - 2\lambda_L^2 Z_{\mathrm{hF}}^2 \frac{4e^2}{\hbar^2}\frac{1}{N}\sum_{\mathbf{k}} \sin^2 k_y [\chi_1 t - 2\chi_2 t' \cos k_x]^2 \times \frac{\beta e^{\beta E_{\mathrm{h}\mathbf{k}}}}{(e^{\beta E_{\mathrm{h}\mathbf{k}}} + 1)^2}. \tag{23}$$

In cuprate superconductors, although the values of J, t, and t' are believed to vary somewhat from compound to compound[4], however, as a qualitative discussion, the commonly used parameters in this paper are chosen as $t/J = 2.5$, $t'/t = 0.3$, and $J = 1000$K. In this case, we plot the effective superfluid density $n_s(T)/n_s(0)$ as a function of temperature T for the doping concentration $\delta = 0.09$ (solid line), $\delta = 0.12$ (dashed line), and $\delta = 0.15$ (dash-dotted line) in Fig. 1. Obviously, it is shown that the effective superfluid density diminishes with increasing temperatures, and disappears at the SC transition temperature T_c, then all the charge carriers are in the normal fluid for the temperature $T \geq T_c$. In summary, we have found the following results within the kinetic energy driven SC mechanism: (1) the doping dependence of the Meissner effect in cuprate superconductors is obtained for all temperature $T \leq T_c$ throughout the SC dome; (2) the electromagnetic response kernel goes to the London form in the long wavelength limit [see Eq. (22)]; (3) although the electromagnetic response kernel is not manifestly gauge invariant within the present bare current vertex (14), it has been shown that the gauge invariance is kept within the dressed current vertex[21].

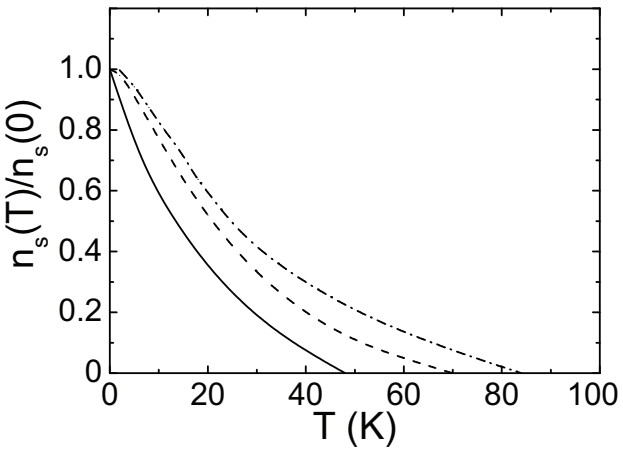

FIG. 1: The effective superfluid density as a function of temperature T for the doping concentration $\delta = 0.09$ (solid line), $\delta = 0.12$ (dashed line), and $\delta = 0.15$ (dash-dotted line) with parameters $t/J = 2.5$, $t'/t = 0.3$, and $J = 1000$K.

III. QUANTITATIVE CHARACTERISTICS OF THE MEISSNER EFFECT

In this section, we discuss the basic behavior of cuprate superconductors in the presence of a weak electromagnetic field. As seen from Eq. (4), once the response kernel $K_{\mu\nu}$ is known, the effect of a weak electromagnetic field can be quantitatively characterized by experimentally measurable quantities such as the local magnetic field profile, the magnetic field penetration depth, and the superfluid density. However, the result we have obtained the response kernel in Eq. (18) [then the effective superfluid density (23)] can not be used for a direct comparison with the corresponding experimental data of cuprate superconductors because the kernel function derived within the linear response theory describes the response of an *infinite* system, whereas in the problem of the penetration of the field and the system has a surface, i.e., it occupies a half-space $x > 0$. In such problems, it is necessary to impose boundary conditions for charge carriers. This can be done within the simplest specular reflection model[35,36] with a two-dimensional geometry of the SC plane. In this case, one may use the response kernel $K_{\mu\nu}$ for an infinite space, however, it is necessary to extend the vector potential $\mathbf{A}(\mathbf{r})$ in an even manner through the boundary. If the externally applied magnetic field is perpendicular to the ab plane, we may choose $A_y(x)$ along the y axis. Following the Maxwell equation,

$$\mathrm{rot}\,\mathbf{B} = \mathrm{rot}\,\mathrm{rot}\,\mathbf{A} = \mathrm{grad}\,\mathrm{div}\,\mathbf{A} - \nabla^2\,\mathbf{A} = \mu_0 \mathbf{J}, \tag{24}$$

it is shown clearly that the extension of the vector potential in an even manner through the boundary implies a kink in the $A_y(x)$ curve. In other words, if the externally applied magnetic field $\mathbf{B}$ is given at the system surface, i.e., $(\mathrm{d}A_y(x)/\mathrm{d}x)|_{x=+0} = B$, while $(\mathrm{d}A_y(x)/\mathrm{d}x)|_{x=-0} = -B$, this leads to a fact[35] that the second derivative $(\mathrm{d}^2A_y(x)/\mathrm{d}^2x)$ acquires a correction $2B\delta(x)$, i.e.,

$$\frac{\mathrm{d}^2 A_y(x)}{\mathrm{d}^2 x} = 2B\delta(x) - \mu_0 J_y, \tag{25}$$

where the transverse gauge $\mathrm{div}\,\mathbf{A} = 0$ has been adopted. In the momentum space, this equation (25) can be expressed as $q_x^2 A_y(\mathbf{q}) = \mu_0 J_y(\mathbf{q}) - 2B$. Substituting this

Fourier transform of Eq. (25) into Eq. (4), and solving for the vector potential we obtain,

$$A_y(\mathbf{q}) = -2B\frac{\delta(q_y)\delta(q_z)}{\mu_0 K_{yy}(\mathbf{q}) + q_x^2}. \quad (26)$$

Since the vector potential has only the y component, the non-zero component of the local magnetic field $\mathbf{h} = \mathrm{rot}\,\mathbf{A}$ is that along the z axis and $h_z(\mathbf{q}) = iq_x A_y(\mathbf{q})$. With the help of Eq. (26), we can obtain explicitly the local magnetic field profile as,

$$h_z(x) = \frac{B}{\pi}\int_{-\infty}^{\infty} \mathrm{d}q_x \frac{q_x \sin(q_x x)}{\mu_0 K_{yy}(q_x, 0, 0) + q_x^2}, \quad (27)$$

which therefore reflects the measurably electromagnetic response in cuprate superconductors. For the convenience in the following discussions, we introduce a characteristic length scale $a_0 = \sqrt{\hbar^2 a/\mu_0 e^2 J}$. Using the lattice parameter $a \approx 0.383$nm for the cuprate superconductor $YBa_2Cu_3O_{7-y}$, this characteristic length is obtain as $a_0 \approx 97.8$nm. In Fig. 2, we plot the local magnetic field profile (27) as a function of the distance from the surface at temperature $T = 2$K for the doping concentration $\delta = 0.09$ (solid line), $\delta = 0.12$ (dashed line), and $\delta = 0.15$ (dash-dotted line) in comparison with the corresponding experimental result[8] of the local magnetic field profiles for the high quality $YBa_2Cu_3O_{7-y}$ (inset). If an external field $B = 8.82$mT is applied to the system just as it has been done in the experimental measurement[8], then the experimental result[8] for $YBa_2Cu_3O_{7-y}$ is well reproduced. In particular, our theoretical results perfectly follow an exponential field decay as expected for the local electrodynamic response. This is different from the conventional superconductors, where the local magnetic field profile in the Meissner state shows a clear deviation from the exponential field decay[8]. The exponential character of the local magnetic field profile has been observed experimentally on different families of cuprate superconductors[7,8], in support of a local (London-type) nature of the electrodynamics[2].

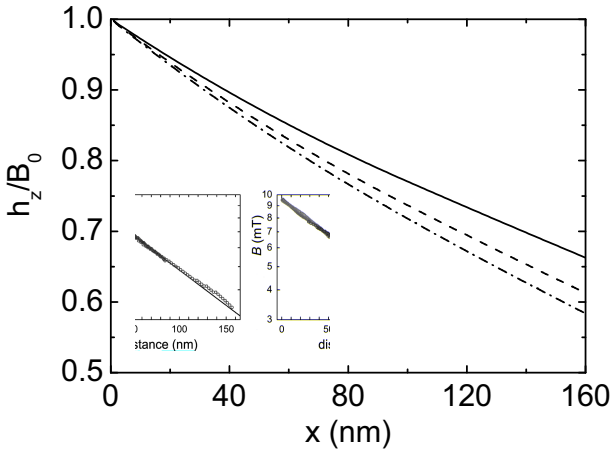

FIG. 2: The local magnetic field profile as a function of the distance from the surface at temperature $T = 2$K for the doping concentration $\delta = 0.09$ (solid line), $\delta = 0.12$ (dashed line), and $\delta = 0.15$ (dash-dotted line) with parameters $t/J = 2.5$, $t'/t = 0.3$, and $J = 1000$K. Inset: the corresponding experimental result for $YBa_2Cu_3O_{7-y}$ taken from Ref. 8.

A. Doping and temperature dependence of the magnetic field penetration depth

In the following discussions, we do not analyze the behavior of the filed in the general case, and only discuss the doping and temperature dependence of the magnetic field in-plane penetration depth $\lambda(T)$ and the related in-plane superfluid density $\rho_s(T)$. The magnetic field in-plane penetration depth is defined in terms of the local magnetic field profile (27) as,

$$\lambda(T) = \frac{1}{B}\int_0^{\infty} h_z(x)\,\mathrm{d}x = \frac{2}{\pi}\int_0^{\infty} \frac{\mathrm{d}q_x}{\mu_0 K_{yy}(q_x, 0, 0) + q_x^2}. \quad (28)$$

At zero-temperature, the calculated magnetic field penetration depths are $\lambda(0) \approx 239.17$nm, $\lambda(0) \approx 234.76$nm, and $\lambda(0) \approx 224.44$nm for the doping concentrations $\delta = 0.14$, $\delta = 0.15$, and $\delta = 0.18$, respectively, which are consistent with the values of the magnetic field penetration depth $\lambda \approx 156$nm ~ 400nm observed for different families of cuprate superconductors in different doping concentrations[7,12–14,37]. On the other hand, at the SC transition temperature $T = T_c$, the kernel of the response function $K_{\mu\nu}(\mathbf{q} \to 0, 0)|_{T=Tc} = 0$. In this case, we obtain the magnetic field penetration depth from Eq. (28) as $\lambda(T_c) = \infty$, which reflects that in the normal state, the external magnetic field can penetrate through the main body of the system, therefore there is no the Meissner effect in the normal state. For a better understanding of the unusual behavior of the temperature dependence of the magnetic field penetration depth $\lambda(T)$, $\Delta\lambda(T) = \lambda(T) - \lambda(0)$ as a function of temperature T for the doping concentration $\delta = 0.14$ (solid line), $\delta = 0.15$ (dashed line), and $\delta = 0.18$ (dash-dotted line) is plotted in Fig. 3 in comparison with the corresponding experimental results[9] of $YBa_2Cu_3O_{7-y}$ (inset). Our result shows clearly that in low temperature, the magnetic field penetration depth $\Delta\lambda(T)$ exhibits a linear temperature dependence, however, it crosses over to a nonlinear behavior in the extremely low temperatures, in good agreement with experimental observation in nominally clean crystals of cuprate superconductors[5,7–11]. In comparison with our previous discussions[21], our present results also show that the good agreement can be reached by introducing the second-nearest neighbors hopping t' in the nearest neighbors hopping t-J model. It should be emphasized that the present result for cuprate superconductors is much different from that in the conventional superconductors, where the characteristic feature is the exis-

tence of the isotropic energy gap Δ_s, and then $\Delta\lambda(T)$ exhibits an exponential behavior as $\Delta\lambda(T) \propto \exp(-\Delta_s/T)$.

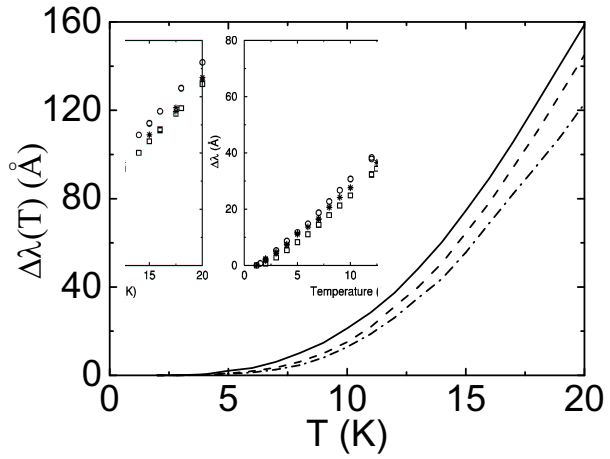

FIG. 3: Temperature dependence of the magnetic field penetration depth $\Delta\lambda(T)$ for the doping concentration $\delta = 0.14$ (solid line), $\delta = 0.15$ (dashed line), and $\delta = 0.18$ (dash-dotted line) with parameters $t/J = 2.5$, $t'/t = 0.3$, and $J = 1000$K. Inset: the corresponding experimental data for $YBa_2Cu_3O_{7-y}$ taken from Ref. 9.

B. Doping and temperature dependence of the in-plane superfluid density

Now we turn to discuss the doping and temperature dependence of the in-plane superfluid density $\rho_{\rm s}(T)$, which is a measure of the phase stiffness, and can be obtained in terms of the magnetic field in-plane penetration depth $\lambda(T)$ as,

$$\rho_{\rm s}(T) \equiv \frac{1}{\lambda^2(T)}. \tag{29}$$

In this case, we have performed firstly a calculation for the doping dependence of the zero-temperature superfluid density $\rho_{\rm s}(0)$ for all levels of doping, and the result is plotted in Fig. 4 in comparison with the corresponding experimental data[13] for $Y_{0.8}Ca_{0.2}Ba_2(Cu_{1-z}Zn_z)_3O_{7-\delta}$ and $Tl_{1-y}Pb_ySr_2Ca_{1-x}Y_xCu_2O_7$ (inset). It is shown clearly that the zero-temperature superfluid density increases with increasing doping in the lower doped regime, and reaches a maximum (a peak) around the critical doping $\delta \approx 0.195$, then decreases in the higher doped regime, in good agreement with the experimental results of cuprate superconductors[12–15]. Since the superfluid density $\rho_{\rm s}(T)$ [then the magnetic field penetration depth $\lambda(T)$] is related to the current-current correlation function, the charge carrier pair gap parameter is relevant as shown in Eqs. (16), (17), and (18), i.e., the variation of the superfluid density with doping and temperature is coupled to the doping and temperature dependence of the charge carrier pair gap parameter $\bar{\Delta}_{hZ}$ in cuprate superconductors. In this case, our present domelike shape of the doping dependent superfluid density also is a natural consequence of the domelike shape of the doping dependence of the SC transition temperature (then the charge carrier pair gap parameter) in the framework of the kinetic energy driven SC mechanism[22], where the the maximal SC transition temperature (then the charge carrier pair gap parameter) occurs in the optimal doping, and then decreases in both underdoped and overdoped regimes. However, the calculated SC transition temperature T_c [then the zero-temperature gap parameter $\bar{\Delta}_{\rm h}(0)$] exhibits the maximal value at the optimal doping $\delta_{\rm optimal} \approx 0.15$[30], therefore there is a difference between the optimal doping $\delta_{\rm optimal} \approx 0.15$ [the maximal $\bar{\Delta}_{\rm h}(0)$ value] and the critical doping $\delta_{\rm critical} \approx 0.195$ [the highest $\rho_{\rm s}(0)$ value]. This difference can be understood within the present theoretical framework. In the domelike shape of the doping dependence of the gap parameter $\bar{\Delta}_{\rm h}(0)$, the gap parameter $\bar{\Delta}_{\rm h}(0)$ reaches its maximal value at the optimal doping $\delta_{\rm optimal} \approx 0.15$, where the doping-derivative of $\bar{\Delta}_{\rm h}(0)$ can be obtained as $({\rm d}\bar{\Delta}_{\rm h}(0)/{\rm d}\delta)|_{\delta=\delta_{\rm optimal}} = 0$. On the other hand, at the critical doping $\delta_{\rm critical} \approx 0.195$, the peak of the superfluid density $\rho_{\rm s}(0)$ appears, where the doping-derivative of $\rho_{\rm s}(0)$ can be obtained as $({\rm d}\rho_{\rm s}(0)/{\rm d}\delta)|_{\delta=\delta_{\rm critical}} = 0$. According to the definition of the superfluid density $\rho_{\rm s}(T)$ in Eq. (29), $({\rm d}\rho_{\rm s}(0)/{\rm d}\delta)|_{\delta=\delta_{\rm critical}} = 0$ is equivalent to $({\rm d}\lambda(0)/{\rm d}\delta)|_{\delta=\delta_{\rm critical}} = 0$. In this case, $({\rm d}\lambda(0)/{\rm d}\delta)|_{\delta=\delta_{\rm critical}} = 0$ can be expressed from Eq. (28) as,

$$\left[\frac{{\rm d}\lambda(0)}{{\rm d}\delta}\right]_{\delta=\delta_{\rm critical}} = -\frac{2\mu_0}{\pi}\int_0^\infty {\rm d}q_{\rm x}\left[\frac{1}{[\mu_0 {\rm K}_{\rm yy}(q_{\rm x},0,0)+q_{\rm x}^2]^2}\frac{{\rm dK}_{\rm yy}(q_{\rm x},0,0)}{{\rm d}\delta}\right]_{\delta=\delta_{\rm critical}} = 0, \tag{30}$$

then with the help of Eqs. (9), (16), and (17), it is straightforward to find that when $({\rm d}\rho_{\rm s}(0)/{\rm d}\delta)|_{\delta=\delta_{\rm critical}} = 0$, $({\rm d}\bar{\Delta}_{\rm h}(0)/{\rm d}\delta)|_{\delta=\delta_{\rm critical}} \neq 0$, since the diamagnetic part of the response kernel in Eq. (9), the spin correlation functions $\chi_1 = \langle S_i^+ S_{i+\hat{\eta}}^-\rangle$ and $\chi_2 = \langle S_i^+ S_{i+\hat{\eta}'}^-\rangle$, and the charge carrier particle-hole parameters $\phi_1 =$

$\langle h^{\dagger}_{i\sigma} h_{i+\hat{\eta}\sigma}\rangle$ and $\phi_2 = \langle h^{\dagger}_{i\sigma} h_{i+\hat{\eta}'\sigma}\rangle$ are also doping dependent. This leads to the difference between the optimal doping $\delta_{\rm optimal} \approx 0.15$ for the zero-temperature gap parameter (then the SC transition temperature) and the critical doping $\delta_{\rm critical} \approx 0.195$ for the zero-temperature superfluid density. In particular, it is found that $({\rm d}\bar{\Delta}_{\rm h}(0)/{\rm d}\delta)|_{\delta=\delta_{\rm critical}} < 0$, indicating that the critical doping locates at the slightly overdoped regime. Furthermore, it should be emphasized that the early experimental data observed from cuprate superconductors show that the superfluid density $\rho_{\rm s}(0)$ in the underdoped regime vanishes more or less linearly with decreasing doping concentration[38]. Later, a clear deviation from this linear relation between the superfluid density $\rho_{\rm s}(0)$ and doping concentration has been observed in the underdoped regime[11–14]. In particular, the recent experimental measurement[15] on the cuprate superconductor $YBa_2Cu_3O_{7-y}$ indicate that the superfluid density $\rho_{\rm s}(0)$ is, in actual fact, linearly proportional to the doping concentration in the low doping range ($\delta \approx 0.054 \sim 0.061$). Our present result in the low doping range also is well consistent with this recent experimental observation[15].

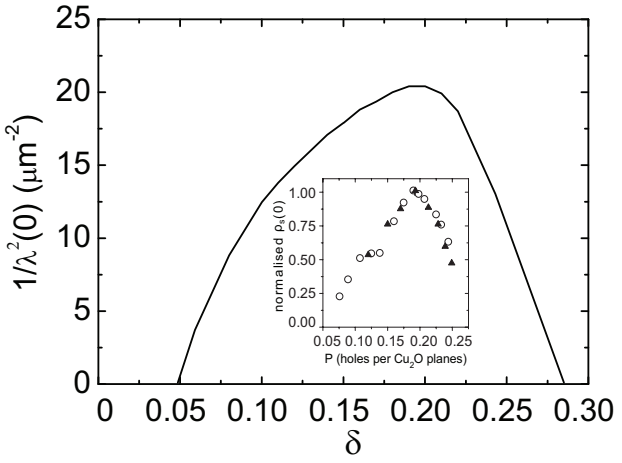

FIG. 4: Doping dependence of the zero-temperature superfluid density with parameters $t/J = 2.5$, $t'/t = 0.3$, and $J = 1000$K. Inset: the corresponding experimental result for $Y_{0.8}Ca_{0.2}Ba_2(Cu_{1-z}Zn_z)_3O_{7-\delta}$ (open circles) and $Tl_{1-y}Pb_ySr_2Ca_{1-x}Y_xCu_2O_7$ (solid triangles) taken from Ref. 13.

The doping dependence of the superfluid density shown in Fig. 4 also is strongly temperature dependent. In particular, when the temperature $T = T_c$, the kernel of the response function $K_{\mu\nu}(\mathbf{q} \to 0, 0)|_{T=Tc} = 0$ and the magnetic field penetration depth $\lambda(T_c) = \infty$ as mentioned in Subsection III A, this leads to the superfluid density $\rho_{\rm s}(T_c) = 0$, which is consistent with the result of the effective superfluid density obtained from Eq. (23). To show the superfluid density clearly for all the temperature $T \leq T_c$, we plot the superfluid density $\rho_{\rm s}(T)$ as a function of temperature for the doping concentration $\delta = 0.06$ (solid line), $\delta = 0.09$ (dashed line), $\delta = 0.12$ (dash-dotted line), and $\delta = 0.15$ (dotted line) in Fig. 5 in comparison with the corresponding experimental result[15] of $YBa_2Cu_3O_{7-y}$ (inset). Our result indicates that the superfluid density $\rho_{\rm s}(T)$ decreases with increasing temperature, and vanishes at the SC transition temperature T_c. Moreover, the most striking feature of the present results is the wide range of linear temperature dependence at low temperature, extending from close to the SC transition temperature T_c to down to the temperatures $T \approx 4$K$\sim$ 8K for different doping concentrations. However, in correspondence with the nonlinear temperature dependence of the magnetic field penetration depth at the extremely low temperatures shown in Fig. 3, the superfluid density $\rho_{\rm s}(T)$ crosses over to a nonlinear temperature behavior at the extremely low temperatures (below $T \approx 4$K$\sim$ 8K for different doping concentrations). Our these results are also well consistent with the corresponding experimental result[12–15] for cuprate superconductors. The good agreement between the present theoretical results and experimental data also shows that the d-wave contribution to the superfluid density $\rho_{\rm s}(T)$ in cuprate superconductors is predominant.

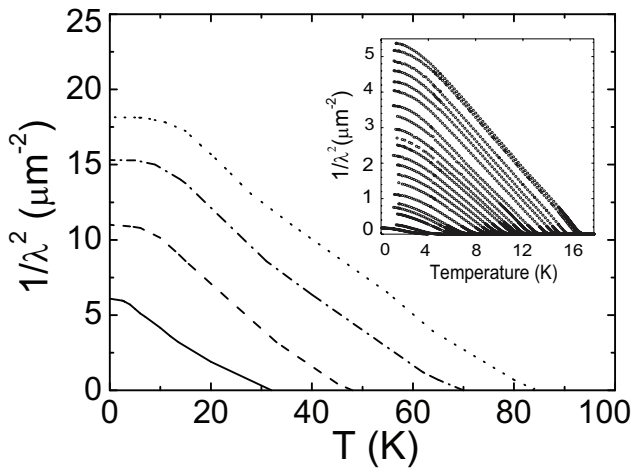

FIG. 5: Temperature dependence of the superfluid density for the doping concentration $\delta = 0.06$ (solid line), $\delta = 0.09$ (dashed line), $\delta = 0.12$ (dash-dotted line), and $\delta = 0.15$ (dotted line) with parameters $t/J = 2.5$, $t'/t = 0.3$, and $J = 1000$K. Inset: the corresponding experimental result for $YBa_2Cu_3O_{7-y}$ taken from Ref. 15.

The essential physics of the nonlinearity in the temperature dependence of the penetration depth (then the superfluid density) in cuprate superconductors at the extremely low temperatures, as shown in Fig. 3 (then Fig. 5), in the present t-t'-J model is the same as that in the t-J[21], and can be attributed to the nonlocal effects induced by the gap nodes on the Fermi surface in a pure d-wave pairing state[16–20]. A weak external magnetic field acts on the SC state of cuprate superconductors as a pertur-

bation. Within the linear response theory, one can find that the nonlocal relation between the supercurrent and the vector potential (4) in the coordinate space holds due to the finite size of Cooper pairs. In particular, in the present kinetic energy driven d-wave SC mechanism[22], the size of charge carrier pairs in the clean limit is of the order of the coherence length $\zeta(\mathbf{k}) = \hbar v_{\rm F}/\pi\Delta_{\rm h}(\mathbf{k})$, where $v_{\rm F} = \hbar^{-1}\partial\xi_{\mathbf{k}}/\partial\mathbf{k}|_{k_F}$ is the charge carrier velocity at the Fermi surface, which shows that the size of charge carrier pairs is momentum dependent. In general, although the external magnetic field decays exponentially on the scale of the magnetic field penetration length $\lambda(T)$, any nonlocal contributions to measurable quantities are of the order of κ^{-2}, where the Ginzburg–Landau parameter κ is the ratio of the magnetic field penetration depth λ and the coherence length ζ. However, for cuprate superconductors, because the pairing is d-wave, the charge carrier gap vanishes on the gap nodes on the Fermi surface, so that the quasiparticle excitations are gapless and therefore affect particularly the physical properties at the extremely low temperatures. This gapless quasiparticle excitation leads a divergence of the coherence length $\zeta(\mathbf{k})$ around the gap nodes on the Fermi surface, and then the behavior of the temperature dependence of the magnetic field penetration depth (then the superfluid density) depends sensitively on the quasiparticle scattering. At the extremely low temperatures, the quasiparticles selectively locate around the gap nodal region, and then the major contribution to measurable quantities comes from these quasiparticles. In this case, the Ginzburg–Landau ratio $\kappa(\mathbf{k})$ around the gap nodal region is no longer large enough for the system to belong to the class of type-II superconductors, and the condition of the local limit is not satisfied[17], which leads to the system in the extreme nonlocal limit, and therefore the nonlinear behavior in the temperature dependence of the magnetic field penetration depth (then superfluid density) is observed experimentally[3,7,8]. On the other hand, with increasing temperature, the quasiparticles around the gap nodal region become excited out of the condensate, and then the nonlocal effect fades away, where the momentum dependent coherence length $\zeta(\mathbf{k})$ can be replaced approximately with the isotropic one $\zeta_0 = \hbar v_{\rm F}/\pi\Delta_{\rm h}$. In this case, the calculated Ginzburg–Landau parameters are $\kappa_0 \approx \lambda(0)/\zeta_0 \approx 166.29$, $\kappa_0 \approx 175.55$, and $\kappa_0 \approx 156.14$ for the doping concentrations $\delta = 0.14$, $\delta = 0.15$, and $\delta = 0.18$, respectively, and therefore the condition for the local limit is satisfied. In particular, these theoretical values of the Ginzburg–Landau parameter in different doping concentrations are very close to the range $\kappa_0 \approx 150 \sim 400$ estimated experimentally for different families of cuprate superconductors in different doping concentrations[7,12–14,37]. As a consequence, our present study shows that cuprate superconductors at moderately low temperatures turn out to be type-II superconductors, where nonlocal effects can be neglected, then the electrodynamics is purely local and the magnetic field decays exponentially over a length of the order of a few hundreds nm.

IV. CONCLUSIONS

Within the t-t'-J model, we have discussed the doping and temperature dependence of the Meissner effect in cuprate superconductors based on the kinetic energy driven SC mechanism. Our results show that in the linear response approach, the electromagnetic response consists of two parts as in the conventional superconductors, the diamagnetic current, which is the acceleration in the magnetic field, and the paramagnetic current, which is a perturbation response of the excited quasiparticle and exactly cancels the diamagnetic term in the normal state, then the Meissner effect is obtained for all the temperature $T \leq T_c$ throughout the SC dome. Within this framework, we have reproduced well all the main features of the doping dependence of the local magnetic field profile, the magnetic field penetration depth, and the superfluid density in terms of the specular reflection model. The local magnetic field profile follows an exponential law, while the magnetic field penetration depth shows a crossover from the linear temperature dependence at low temperatures to a nonlinear one at the extremely low temperatures. Moreover, in analogy to the domelike shape of the doping dependent SC transition temperature, the superfluid density increases with increasing doping in the lower doped regime, and reaches a maximum around the critical doping $\delta \approx 0.195$, then decreases in the higher doped regime. The good agreement between the present theoretical results in the clean limit and experimental data for different families of cuprate superconductors also provides an important confirmation of the nature of the SC phase of cuprate superconductors as a d-wave BCS-like SC state within the kinetic energy driven SC mechanism.

Finally, it should be emphasized that in the present study, the only coupling of the electron charge to the weak external magnetic field is considered in terms of the vector potential $\mathbf{A}$, while the coupling of the electron magnetic momentum with the weak external magnetic field in terms of the Zeeman mechanism has been dropped. In this case, the above obtained results are only valid in the weak external magnetic field limit. However, the depairing due to the Pauli spin polarization is very important in the presence of a moderate or strong external magnetic field, since cuprate superconductors are doped Mott insulators with the strong short-range antiferromagnetic correlation dominating the entire SC phase[4]. In particular, in the the kinetic energy driven SC mechanism[22], where the charge carrier-spin interaction from the kinetic energy term induces a d-wave pairing state by exchanging spin excitations. Therefore under the kinetic energy driven SC mechanism, a moderate or strong external magnetic field aligns the spins of the unpaired electrons, then the d-wave electron Cooper pairs in cuprate superconductors can not take advantage of the lower energy offered by a spin-polarized state[39]. In

this case, we[40] have studied the magnetic field dependence of the superfluid density and doping dependence of the upper critical magnetic field in cuprate superconductors for all the temperature $T \leq T_c$ throughout the SC dome by considering both couplings of the electron charge and electron magnetic momentum with a moderate and a strong external magnetic field, respectively, and the results show that the external magnetic field inducing an reduction of the low-temperature superfluid density, while the maximal upper critical magnetic field occurs around the optimal doping, and then decreases in both underdoped and overdoped regimes, in qualitative agreement with the corresponding experimental data[41,42]. These and the related results will be presented elsewhere.

Acknowledgments

The authors would like to thank Dr. M. Krzyzosiak and Professor Y. J. Wang for helpful discussions. This work was supported by the National Natural Science Foundation of China under Grant No. 10774015, and the funds from the Ministry of Science and Technology of China under Grant Nos. 2006CB601002 and 2006CB921300.

Appendix A: Paramagnetic response kernel at zero-temperature and superconducting transition temperature

In this Appendix, we discuss the paramagnetic part of the response kernel in Eq. (19) in the long wavelength limit at the zero-temperature ($T = 0$) and SC transition temperature ($T = T_c$). Firstly, we discuss the case at $T = 0$. In the long wavelength limit, i.e., $|\mathbf{q}| \to 0$, the paramagnetic part of the response kernel (19) can be evaluated as,

$$K_{yy}^{(\mathrm{p})}(\mathbf{q}\to 0,0)|_{T\to 0} = -2Z_{\mathrm{hF}}^2\frac{4e^2}{\hbar^2}\left[\frac{1}{N}\sum_{\mathbf{k}}\sin^2 k_y[\chi_1 t-2\chi_2 t'\cos k_x]^2\frac{\beta e^{\beta E_{\mathrm{h}\mathbf{k}}}}{(e^{\beta E_{\mathrm{h}\mathbf{k}}}+1)^2}\right]_{T\to 0} \tag{A1}$$

where $N = N_x N_y$, N is the number of sites on a square lattice, while N_x and N_y are corresponding numbers of sites in the $\hat{x}$ and $\hat{y}$ directions, respectively. In the d-wave pairing state, the characteristic feature is that the energy gap vanishes $\Delta_{\mathrm{h}}(\mathbf{k})|_{|k_x|=|k_y|} = \Delta_{\mathrm{h}}(\cos k_x - \cos k_y)/2|_{|k_x|=|k_y|} = 0$ along the diagonal directions in the Brillouin zone. In this case, the paramagnetic part of the response kernel in Eq. (A1) can be rewritten as,

$$\begin{aligned} K_{yy}^{(\mathrm{p})}(\mathbf{q}\to 0,0)|_{T\to 0} &= -2Z_{\mathrm{hF}}^2\frac{4e^2}{\hbar^2}\left[\frac{1}{N}\sum_{\mathbf{k}(|k_x|\neq|k_y|)}\sin^2 k_y[\chi_1 t-2\chi_2 t'\cos k_x]^2\frac{\beta e^{\beta E_{\mathrm{h}\mathbf{k}}}}{(e^{\beta E_{\mathrm{h}\mathbf{k}}}+1)^2}\right]_{T\to 0} \\ &- 2Z_{\mathrm{hF}}^2\frac{4e^2}{\hbar^2}\frac{1}{N_x}\left[\frac{1}{N_y}\sum_{k_y}\sin^2 k_y[\chi_1 t-2\chi_2 t'\cos k_y]^2\frac{\beta e^{\beta\bar{\xi}_{k_y}}}{(e^{\beta\bar{\xi}_{k_y}}+1)^2}\right]_{T\to 0} \end{aligned} \tag{A2}$$

where $\bar{\xi}_{k_y} = Z_{\mathrm{hF}}(Zt\chi_1\cos k_y - Zt'\chi_2\cos^2 k_y - \mu)$. The first term of the right-hand side is equal to zero since the existence of the gap, while the second term of the right-hand side can be evaluated explicitly as,

$$\begin{aligned} &- 2Z_{\mathrm{hF}}^2\frac{4e^2}{\hbar^2}\frac{1}{N_x}\left[\int_{-\pi}^{\pi}\frac{dk_y}{2\pi}\sin^2 k_y[\chi_1 t-2\chi_2 t'\cos k_y]^2\frac{\beta e^{\beta\bar{\xi}_{k_y}}}{(e^{\beta\bar{\xi}_{k_y}}+1)^2}\right]_{T\to 0} \\ &= \frac{2Z_{\mathrm{hF}}}{Z}\frac{4e^2}{\hbar^2}\frac{1}{N_x}\left[\int_{-\pi}^{\pi}\frac{dk_y}{2\pi}[\chi_1 t\cos k_y - 2\chi_2 t'\cos(2k_y)]\frac{1}{e^{\beta\bar{\xi}_{k_y}}+1}\right]_{T\to 0} \\ &= \frac{2Z_{\mathrm{hF}}}{Z}\frac{4e^2}{\hbar^2}\frac{1}{N_x}\left[\int_{-\pi}^{\pi}\frac{dk_y}{2\pi}[\chi_1 t\cos k_y - 2\chi_2 t'\cos(2k_y)]\theta(\bar{\xi}_{k_y})\right], \end{aligned} \tag{A3}$$

which is equal to zero in the thermodynamic limit $N \to \infty$ (then $N_x \to \infty$ and $N_y \to \infty$), where the step function $\theta(x) = 1$ for $x < 0$ and $\theta(x) = 0$ for $x > 0$.

Now we turn to discuss the paramagnetic part of the response kernel (19) in the long wavelength limit at $T = T_c$ ($\beta_c = T_c^{-1}$). In this case, the energy gap $\bar{\Delta}_{\mathrm{hZ}}(\mathbf{k})|_{T=T_c} = 0$, and the paramagnetic part of the response kernel (19) can

be evaluated explicitly as,

$$\begin{aligned} K_{yy}^{(\mathrm{p})}(\mathbf{q}\to 0,0) &= -2Z_{\mathrm{hF}}^2\frac{4e^2}{\hbar^2}\frac{1}{N}\sum_{\mathbf{k}}\sin^2 k_y[\chi_1 t-2\chi_2 t'\cos k_x]^2\frac{\beta_c e^{\beta_c\bar{\xi}_{\mathbf{k}}}}{(e^{\beta_c\bar{\xi}_{\mathbf{k}}}+1)^2} \\ &= -2Z_{\mathrm{hF}}^2\frac{4e^2}{\hbar^2}\int_{-\pi}^{\pi}\frac{dk_x}{2\pi}\int_{-\pi}^{\pi}\frac{dk_y}{2\pi}\sin^2 k_y[\chi_1 t-2\chi_2 t'\cos k_x]^2\frac{\beta_c e^{\beta_c\bar{\xi}_{\mathbf{k}}}}{(e^{\beta_c\bar{\xi}_{\mathbf{k}}}+1)^2} \\ &= Z_{\mathrm{hF}}\frac{4e^2}{\hbar^2}\int_{-\pi}^{\pi}\frac{dk_x}{2\pi}\int_{-\pi}^{\pi}\frac{dk_y}{2\pi}[\chi_1 t\cos k_y-2\chi_2 t'\cos k_x\cos k_y]\frac{1}{e^{\beta_c\bar{\xi}_{\mathbf{k}}}+1} \\ &= Z_{\mathrm{hF}}\frac{4e^2}{\hbar^2}\frac{1}{N}\sum_{\mathbf{k}}[\chi_1 t\cos k_y-2\chi_2 t'\cos k_x\cos k_y]n_F(\bar{\xi}_{\mathbf{k}}) = \frac{4e^2}{\hbar^2}[\chi_1\phi_1 t-2\chi_2\phi_2 t'] = -\frac{1}{\lambda_L^2}, \quad \text{(A4)} \end{aligned}$$

which exactly cancels the diamagnetic part of the response kernel in Eq. (9), then the Meissner effect is obtained for all $T \le T_c$ throughout the SC dome.

* To whom correspondence should be addressed.

[2] See, e.g., J. R. Schrieffer, *Theory of Superconductivity* (Addison-Wesley, San Francisco, 1964).

[3] See, e.g., B. A. Bonn and W. N. Hardy, in *Physical Properties of High Temperature Superconductors* V, edited by D. M. Ginsberg (World Scientific, Singapore, 1996).

[4] See, e.g., A. Damascelli, Z. Hussain, and Z.-X. Shen, Rev. Mod. Phys. **75**, 473 (2003).

[5] W. N. Hardy, D. A. Bonn, D. C. Morgan, Ruixing Liang, and Kuan Zhang, Phys. Rev. Lett. **70**, 3999 (1993).

[6] See, e.g., C. C. Tsuei and J. R. Kirtley, Rev. Mod. Phys. **72**, 969 (2000).

[7] R. Khasanov, D. G. Eshchenko, H. Luetkens, E. Morenzoni, T. Prokscha, A. Suter, N. Garifianov, M. Mali, J. Roos, K. Conder, and H. Keller, Phys. Rev. Lett. **92**, 057602 (2004).

[8] A. Suter, E. Morenzoni R. Khasanov, H. Luetkens, T. Prokscha, and N. Garifianov, Phys. Rev. Lett. **92**, 087001 (2004).

[9] S. Kamal, Ruixing Liang, A. Hosseini, D. A. Bonn, and W. N. Hardy, Phys. Rev. B. **58**, R8933 (1998).

[10] T. J. Jackson, T. M. Riseman, E. M. Forgan, H. Glückler, T. Prokscha, E. Morenzoni, M. Pleines, Ch. Niedermayer, G. Schatz, H. Luetkens, and J. Litterst, Phys. Rev. Lett. **84**, 4958 (2000); Kuan Zhang, D. A. Bonn, S. Kamal, Ruixing Liang, D. J. Baar, W. N. Hardy, D. Basov, and T. Timusk, Phys. Rev. Lett. **73**, 2484 (1994); Jian Mao, D. H. Wu, J. L. Peng, R. L. Greene, and Steven M. Anlage, Phys. Rev. B **51**, 3316 (1995).

[11] T. Jacobs, S. Sridhar, Qiang Li, G. D. Gu, and N. Koshizuka, Phys. Rev. Lett. **75**, 4516 (1995); Shih-Fu Lee, D. C. Morgan, R. J. Ormeno, D. M. Broun, R. A. Doyle, J. R. Waldram, and K. Kadowaki, Phys. Rev. Lett. **77**, 735 (1996); C. Panagopoulos, J. R. Cooper, G. B. Peacock, I. Gameson, P. P. Edwards, W. Schmidbauer, and J. W. Hodby, Phys. Rev. B **53**, R2999 (1996); T. Pereg-Barnea, P. J. Turner, R. Harris, G. K. Mullins, J. S. Bobowski, M. Raudsepp, Ruixing Liang, D. A. Bonn, and W. N. Hardy, Phys. Rev. B **69**, 184513 (2004).

[12] Ch. Niedermayer, C. Bernhard, U. Binninger, H. Glückler, J. L. Tallon, E. J. Ansaldo, and J. I. Budnick, Phys. Rev. Lett. **71**, 1764 (1993); L. Fábrega, A. Calleja, A. Sin, S. Piñol, X. Obradors, J. Fontcuberta, and P. J. C. King, Phys. Rev. B **60**, 7579 (1999); J. L. Tallon, J. W. Loram, J. R. Cooper, C. Panagopoulos, and C. Bernhard, Phys. Rev. B **68**, 180501 (2003).

[13] C. Bernhard, J. L. Tallon, Th. Blasius, A. Golnik, and Ch. Niedermeyer, Phys. Rev. Lett. **86**, 1614 (2001).

[14] C. Panagopoulos, B. D. Rainford, J. R. Cooper, W. Lo, J. L. Tallon, J. W. Loram, J. Betouras, Y. S. Wang, and C. W. Chu, Phys. Rev. B. **60**, 14617 (1999); R. Khasanov, Takeshi Kondo, M. Bendele, Yoichiro Hamaya, A. Kaminski, S. L. Lee, S. J. Ray, Tsunehiro Takeuchi, arXiv:1004.1275 (unpublished).

[15] D. M. Broun, W. A. Huttema, P. J. Turner, S. Özcan, B. Morgan, Ruixing Liang, W. N. Hardy, and D. A. Bonn, Phys. Rev. Lett. **99**, 237003 (2007).

[16] S. K. Yip and J. Sauls, Phys. Rev. Lett. **69**, 2264 (1992).

[17] I. Kosztin and A. J. Legget, Phys. Rev. Lett. **79**, 135 (1997).

[18] M. Franz, I. Affleck, and M. H. S. Amin, Phys. Rev. Lett. **79**, 1555 (1997); M. H. S. Amin, M. Franz, and I. Affleck, Phys. Rev. Lett. **84**, 5864 (2000).

[19] Mei-Rong Li, P. J. Hirschfeld, and P. Wölfle, Phys. Rev. B **61**, 648 (2000).

[20] D. E. Sheehy, T. P. Davis, and M. Franz, Phys. Rev. B **70**, 054510 (2004).

[21] Mateusz Krzyzosiak, Zheyu Huang, Shiping Feng, and Ryszard Gonczarek, Physica C **470**, 407 (2010).

[22] Shiping Feng, Phys. Rev. B **68**, 184501 (2003); Shiping Feng, Tianxing Ma, and Huaiming Guo, Physica C **436**, 14 (2006).

[23] B. O. Well, Z.-X. Shen, A. Matsuura, D. M. King, M. A. Kastner, M. Greven, and R. J. Birgeneau, Phys. Rev. Lett. **74**, 964 (1995); C. King, P. J. White, Z.-X. Shen, T. Tohyama, Y. Shibata, S. Maekawa, B. O. Wells, Y. J. Kim, R. J. Birgeneau, and M. A. Kastner, Phys. Rev. Lett. **80**, 4245 (1998).

[24] K. Tanaka, T. Yoshida, A. Fujimori, D. H. Lu, Z.-X. Shen, X.-J. Zhou, H. Eisaki, Z. Hussain, S. Uchida, Y. Aiura, K. Ono, T. Sugaya, T. Mizuno, and I. Terasaki, Phys. Rev. B **70**, 092503 (2004).

[25] P. W. Anderson, in: *Frontiers and Borderlines in Many Particle Physics*, edited by R. A. Broglia and J. R. Schrieffer (North-Holland, Amsterdam, 1987), p. 1; Science **235**, 1196 (1987).

[26] J. E. Hirsch and F. Marsiglio, Phys. Rev. B **45**, 4807 (1992); D. J. Scalapino, S. R. White, and S. C. Zhang, Phys. Rev. Lett. **68**, 2830 (1992); Phys. Rev. B **47**, 7995 (1993); T. Kostyrko, R. Micnas, and K. A. Chao, Phys. Rev. B **49**, 6158 (1994).

[27] S. Misawa, Phys. Rev. B **49**, 6305 (1994).

[28] Shiping Feng, Jihong Qin, and Tianxing Ma, J. Phys.: Condens. Matter **16**, 343 (2004).

[29] See, e.g., the review, Shiping Feng, Huaiming Guo, Yu Lan, and Li Cheng, Int. J. Mod. Phys. B **22**, 3757 (2008).

[30] Huaiming Guo and Shiping Feng, Phys. Lett. A **361**, 382 (2007).

[31] See, e.g., A. L. Fetter and J. D. Walecka, *Quantum Theory of Many-Particle Systems* (McGraw-Hill, 1971) Sec. 13.52.

[32] H. Fukuyama, H. Ebisawa, and Y. Wada, Prog. Theor. Phys. **42**, 494 (1969); H. Fukuyama, Prog. Theor. Phys. **42**, 1284 (1969).

[33] See, e.g., G. D. Mahan, *Many-Particle Physics*, (Plenum Press, New York, 1981).

[34] R. B. Laughlin, Phys. Rev. Lett. **79**, 1726 (1997); J. Low. Tem. Phys. **99**, 443 (1995).

[35] See, e.g., A. A. Abrikosov, *Fundamentals of the Theory of Metals* (Elsevier Science Publishers B. V., 1988).

[36] See, e.g., M. Tinkham, *Introduction to Superconductivity* (McGraw-Hill, 1996) Appendix 3.

[37] Y. J. Uemura, A. Keren, L. P. Le, G. M. Luke, W. D. Wu, Y. Kubo, T. Manako, Y. Shimakawa, M. Subramanian, J. L. Cobb, and J. T. Markert, Nature **364**, 605 (1993); M. Nideröst, R. Frassanito, M. Saalfrank, A. C. Mota, G. Blatter, V. N. Zavaritsky, T. W. Li, and P. H. Kes, Phys. Rev. Lett. **81**, 3231 (1998); S. L. Lee, P. Zimmermann, H. Keller, M. Warden, I. M. Savić, R. Schauwecker, D. Zech, R. Cubitt, E. M. Forgan, P. H. Kes, T. W. Li, A. A. Menovsky, and Z. Tarnawski, Phys. Rev. Lett. **71**, 3862 (1993).

[38] Y. Uemura, G. M. Luke, B. J. Sternlieb, J. H. Brewer, J. F. Carolan, W. N. Hardy, R. Kadono, J. R. Kempton, R. F. Kiefl, S. R. Kreitzman, P. Mulhern, T. M. Riseman, D. Ll. Williams, B. X. Yang, S. Uchida, H. Takagi, J. Gopalakrishnan, A. W. Sleight, M. A. Subramanian, C. L. Chien, M. Z. Cieplak, Gang Xiao, V. Y. Lee, B. W. Statt, C. E. Stronach, W. J. Kossler, and X. H. Yu, Phys. Rev. Lett. **62**, 2317 (1989); Y. J. Uemura, L. P. Le, G. M. Luke, B. J. Sternlieb, W. D. Wu, J. H. Brewer, T. M. Riseman, C. L. Seaman, M. B. Maple, M. Ishikawa, D. G. Hinks, J. D. Jorgensen, G. Saito, and H. Yamochi, Phys. Rev. Lett. **66**, 2665 (1991).

[39] A. B. Vorontsov and I. Vekhter, Phys. Rev. B **81**, 094527 (2010).

[40] Zheyu Huang, Huaisong Zhao, and Shiping Feng, unpublished.

[41] J.E. Sonier, J.H. Brewer, R.F. Kiefl, G.D. Morris, R. Miller, D.A. Bonn, J. Chakhalian, R.H. Heffner, W.N. Hardy, and R. Liang, Phys. Rev. Lett. **83** (1999) 4156; R. Khasanov, Takeshi Kondo, S. Strässle, D. O. G. Heron, A. Kaminski, H. Keller, S. L. Lee, and Tsunehiro Takeuchi, Phys. Rev. B **79** (2009) 180507 (R).

[42] Y. Wang and H.-H. Wen, Europhys. Lett. **81** (2008) 57007.